

---

# Breaking MLPerf Training: A Case Study on Optimizing BERT

---

Yongdeok Kim<sup>1</sup> Jaehyung Ahn<sup>1</sup> Myeongwoo Kim<sup>1</sup> Changin Choi<sup>1</sup>  
Heejae Kim<sup>1</sup> Narankhuu Tuvshinjargal<sup>1</sup> Seungwon Lee<sup>1</sup> Yanzi Zhang<sup>2</sup>  
Yuan Pei<sup>2</sup> Xiongzhan Linghu<sup>2</sup> Jingkun Ma<sup>2</sup> Lin Chen<sup>2</sup>  
Yuehua Dai<sup>2</sup> Sungjoo Yoo<sup>3</sup>

<sup>1</sup>Samsung Advanced Institute of Technology <sup>2</sup>Samsung R&D Institute China Xian  
<sup>3</sup>Seoul National University

{yd.mlg.kim, jh91.ahn, k.myeong-woo, ci2015.choi,  
heejaeee.kim, nate.tuvshin, seungw.lee, yanzi.zhang,  
yuan.pei, xz.linghu, jingkun.ma, lin81.chen, yuehua.dai}@samsung.com  
sungjoo.yoo@gmail.com

## Abstract

Speeding up the large-scale distributed training is challenging in that it requires improving various components of training including load balancing, communication, optimizers, etc. We present novel approaches for fast large-scale training of BERT model which individually ameliorates each component thereby leading to a new level of BERT training performance. Load balancing is imperative in distributed BERT training since its training datasets are characterized by samples with various lengths. Communication cost, which is proportional to the scale of distributed training, needs to be hidden by useful computation. In addition, the optimizers, e.g., ADAM, LAMB, etc., need to be carefully re-evaluated in the context of large-scale distributed training. We propose two new ideas, (1) local presorting based on dataset stratification for load balancing and (2) bucket-wise gradient clipping before allreduce which allows us to benefit from the overlap of gradient computation and synchronization as well as the fast training of gradient clipping before allreduce. We also re-evaluate existing optimizers via hyperparameter optimization and utilize ADAM, which also contributes to fast training via larger batches than existing methods. Our proposed methods, all combined, give the fastest MLPerf BERT training of 25.1 (22.3) seconds on 1,024 NVIDIA A100 GPUs, which is  $1.33\times$  ( $1.13\times$ ) and  $1.57\times$  faster than the other top two (one) submissions to MLPerf v1.1 (v2.0). Our implementation and evaluation results are available at MLPerf v1.1~v2.1.

## 1 Introduction

Although large-scale data-parallel training has been actively studied in recent years, there is still a large room for improvements in making best use of extremely large-scale GPU resources. Especially, due to the ever-increasing training cost, it is imperative to improve its efficiency, i.e., faster training. Load balancing and communication/computation overlapping are two most important factors which affect efficiency. We investigate these two issues in the training of the representative model, BERT on a large-scale GPU training system consisting of 1,024 NVIDIA A100 GPUs with 100 GB/s network bandwidth.

Load balancing of large-scale data-parallel training of language models is challenging due to the fact that NLP datasets, used in BERT pre-training, are characterized by the diversity in input data size. It is mainly because the training datasets are obtained by collecting texts from various sources, e.g., web

pages, books, news articles, etc. and these texts tend to exhibit wide distributions in terms of sequence length. Such a large variation in sequence lengths can incur a significant load imbalance across GPUs thereby degrading the training speed. For instance, a BERT model of sequence length 512 wastes almost half the computation budget due to padded tokens to short sentences in the Wikipedia dataset [4]. Recently, a few studies have been presented to address this problem. In [15], the training data are first sorted in terms of sequence length and balanced batches are formed by utilizing the sorted sequences. Krell *et al.* [4] propose a novel packing method, which addresses this problem and shows that a maximum  $2\times$  speedup is achievable. These existing methods show a potential of improving training speed through better load balancing. However, each incurs new overhead, e.g., allgather and sorting the training dataset [15], or loses advantages in case of large batches, e.g., the benefit of CUDA graph cannot be exploited in local batches larger than 6 due to the lack of memory. Furthermore, the packing method does not preserve the order of sentences, so it is impossible to use the packing method for tasks such as question-answer, where the order of the sentences is important.

In standard data-parallel training, overlapping computation and communication between compute devices is typically realized by overlapping backward pass (i.e., gradient computation on individual GPUs in parallel) and gradient synchronization (i.e., allreduce via inter-GPU communication). The communication and computation is overlapped in a fine-grained manner. Specifically, a bucket of gradients is communicated across GPUs while the next bucket of gradients is being computed on each GPU. To further improve training efficiency, i.e., via fewer iterations of training, we investigated the possibility of adopting sophisticated training methods in the standard data-parallel training. Especially, although gradient clipping before allreduce can accelerate training, it has not been adopted in the data-parallel training since it cannot benefit from the communication/computation overlapping due to its requirement of performing gradient clipping (involving inter-GPU communication) before allreduce and the resulting serialization of computations (gradient computation and clipping) and synchronization (allreduce).

In this paper, we address two problems of load balancing and overlapping and propose novel ideas for improving the training speed of large-scale data-parallel BERT training. In addition, we revisit the selection of optimizers in the context of large-scale distributed BERT training and select ADAM as the optimizer, enabling us to utilize larger batches than the other optimizers while finally contributing to fast training.

Our contributions are summarized as follows:

- We investigate the characteristics of training datasets in NLP training and propose a novel and low-cost method of forming balanced batches based on stratification and local presorting.
- In order to address the problem of no overlapping between communication and computation in gradient clipping before allreduce, we propose performing gradient clipping in a bucket-wise manner, which is critical for us to achieve the SOTA training speed in BERT training.
- We also demonstrate the conventional ADAM is still effective in large-scale BERT training under hyperparameter optimization and can contribute to fast training with large batches.

## 2 Background

### 2.1 Data Parallelism

Data parallelism plays a critical role in training models with large parameters and/or large training data on large-scale compute devices, e.g., GPUs. In data parallelism, whether it is adopted in a purely data-parallel setting or used together with other types of parallelism, e.g., model/pipeline parallelism [11], each GPU first stores its own copy of the entire model in the beginning of training (in a purely data-parallel setting of small model training) or prepares the model parameters of each layer, on the fly, via allgather under ZeRO [11] (for large model training). Each GPU performs forward and backward passes of training. The local gradients obtained in the backward pass are exchanged across GPUs in order for each GPU to update its copy of the entire model. There have been many studies to improve the performance of data-parallel training: synchronous (i.e., weight update in every iteration of training) vs. asynchronous weight updates, parameter server vs. allreduce, gradient compression, etc. [19]. These days, thanks to two key innovations to be briefly explained below, a typical choice is synchronous allreduce without gradient compression when adequate network bandwidth is available [1].

**Allreduce** There have been various optimizations of allreduce such as ring-reduce [2], tree-reduce [17], recursive doubling [20], etc. The optimizations are tightly coupled with the underlying communication networks (topology and bandwidth), which makes it difficult to optimize allreduce on a given large-scale training platform consisting of thousands of GPUs connected by a complicated network. However, recent solutions such as NCCL from NVIDIA dynamically selects suitable options, e.g., between double binary-tree-reduce and ring-reduce, considering the number of GPUs, and the topology, bandwidth and unit size of communication.

**Communication and computation overlap** In the backward pass of training, while the current gradients are being computed, the previously calculated gradients can be synchronized, i.e., allreduce can be performed on them across GPUs in order for each GPU to obtain the final updates to the model parameters (copied across the GPUs). Such a capability of hiding communication with computation is one of the key requirements for efficient data-parallel training. The collective communication of allreduce is often realized at the granularity of bucket (e.g., 25 MB by default in PyTorch) in order to amortize the overhead of calling allreduce collectives. It is crucial to realize efficient allreduce collectives by dynamically ordering buckets while tracing the backward order using autograd hooks and updating parameters according to bucket mapping [6, 18].

## 2.2 Large Batch Training

Large batch training, which is required to make the best use of large-scale compute resources, is known to suffer from lack of generalization ability. Krizhevsky proposes a simple heuristics that increases the learning rate in proportion to the batch size and this strategy works up to a certain batch size [5]. You *et al.* propose a layer-wise adaptive rate scaling method that scales parameter updates by the  $L_2$  norm of parameters [24]. You *et al.* also propose LAMB method that combines the layer-wise adaptive rate scaling with ADAM, which enables large batch training for BERT and ResNet50 models [25]. It is also reported that, under sufficient hyperparameter optimizations, the standard optimizers like ADAM can offer even better results in large batch training. In this work, as explained later, we also conducted hyperparameter optimizations and found ADAM works best [25]. Thus, all the key results of our experiments were obtained using ADAM optimizer.

## 2.3 Gradient Clipping

Gradient clipping, which is to scale the gradient if it gets too large, is widely adopted for improving training. In this paper, we apply clipping-by-norm which is defined as follows. If  $\|\mathbf{g}\| \geq c$  then

$$\mathbf{g} \leftarrow c \cdot \mathbf{g} / \|\mathbf{g}\|,$$

where threshold  $c$  is typically set to 1 and  $\|\mathbf{g}\|$  is the norm of the gradients  $\mathbf{g}$ . The gradient scale is usually applied to the entire gradients of a layer. Thus, it can be computed when all the gradients are calculated, which means clipping needs to be applied before or after allreduce. Although clipping before allreduce proves more effective than clipping after allreduce, it is not usually adopted since we cannot overlap gradient computation and synchronization in gradient clipping before allreduce. In this paper, we propose a novel method to enable both gradient clipping before allreduce and communication/synchronization overlapping.

## 2.4 BERT Training in MLPerf Benchmark

BERT training consists of two phases: (1) training from a random initialization with short sequences (at lengths of  $<128$ ) to a certain accuracy and (2) training with longer sequences ( $<512$ ) from the same checkpoint to a target accuracy. MLPerf benchmark adopts only the second phase since the training from the same checkpoint to a certain target accuracy level (72.0%) enables fair and effective comparisons. Even though our experiments are performed only for the MLPerf benchmark for a few seconds, our methods can be applied to the entire training process and thus make a high contribution to training efficiency. [9]

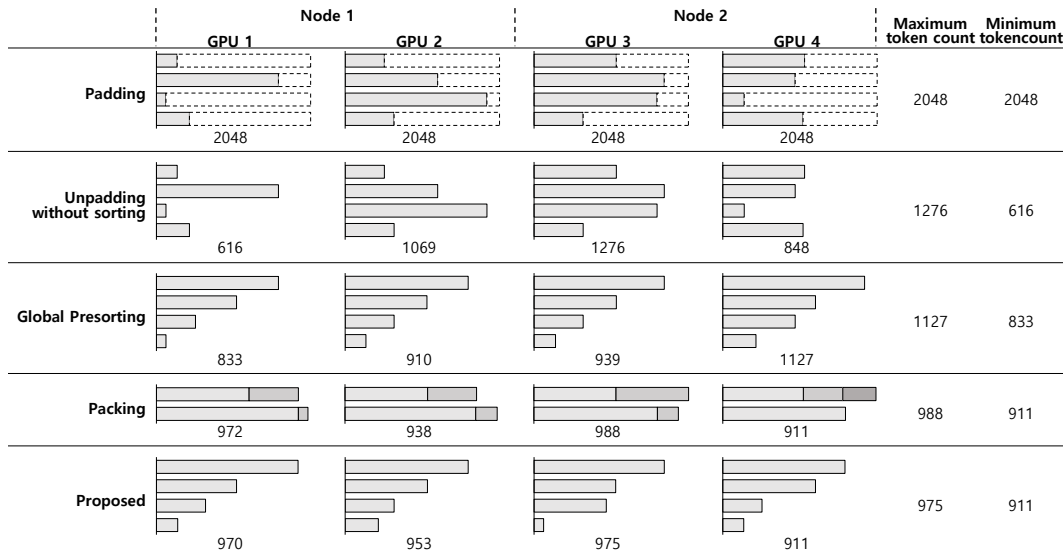


Figure 1. Illustrative comparison of load balancing. Each horizontal bar represents a sequence and its length is proportional to the number of tokens of the sequence. Numbers below bars represent per-GPU token counts, i.e., the total sum of sample token counts processed by the associated GPU. Larger difference between maximum and minimum token count implies higher imbalance.

### 3 Motivation

#### 3.1 Irregular Sequence Length in NLP Datasets

The sequence length distribution of NLP datasets is characterized by a skewed distribution. For example, in the Wikipedia dataset [23], the percentages of data with sequence lengths of 1 to 128, 129 to 256, 257 to 348, and 349 to 512 are 37.3%, 19.7%, 11.7%, and 31.4%, respectively. It is reported that SQUAD [16] and GLUE [21] also have similar skewed distributions [4]. The conventional method of handling irregular sequence length in batch-based training is zero padding. In such a case, if a simple zero padding is adopted, approximately 50% of GEMM computation is wasted due to matrix multiplication with the padded zero values [4].

Figure 1 illustrates the wasted computation due to zero padding, and three existing methods to address this problem. In the figure, the padding case does not have load imbalance problem, but it suffers from low utilization of compute resource due to the wasted computation denoted with dashed rectangles. The unpadding case illustrates the effect of recently available unpadding method which performs only the necessary computation with the given input sequence [26].

That is, it skips the computation of zero padding input in the padding case. In such a case, as the figure shows, the total amount of computation can be significantly reduced. However, the load imbalance across GPUs (the ratio of maximum to minimum per-GPU token count) is still large, 2.07.

In the case of unpadding with global presorting [15], the load imbalance can be mitigated as shown in the figure. It gathers all the input samples of a batch, sort them in terms of sample length, and allocate them to GPUs in the sorted order. Thus, the variation of the per-GPU token counts can be reduced thereby improving the imbalance in the example. However, this method incurs an additional cost of global sorting which involves communication across all the GPUs.

The figure shows that packing [4] can further improve load balance. It is to allow the allocation of more than one samples to the input sequence (of the BERT model). As the figure illustrates, packing has a potential of offering well-balanced sample allocations across GPUs.

The figure also illustrates the effect of our proposed method which, unlike global presorting, does not incur the cost of global communication, but instead performs local sorting on a GPU basis. As exemplified in the figure, it has a potential of obtaining well-balanced sample allocation across GPUs based on the dataset stratification.

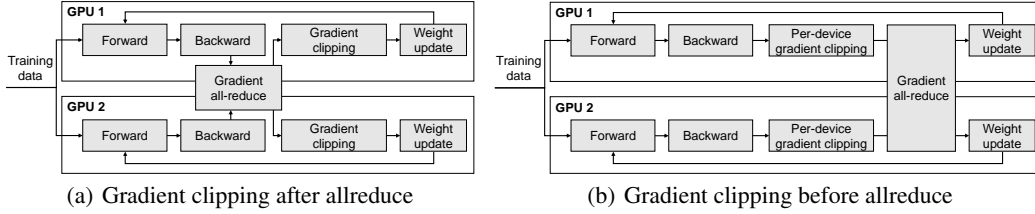


**Figure 2. An illustration of two possible ways to implement gradient clipping in distributed training: (a) gradient clipping after allreduce and (b) gradient clipping before allreduce.**

### 3.2 Gradient Clipping After/Before AllReduce

Figure 2 illustrates two ways of gradient clipping: clipping after/before allreduce. As the figure shows, gradient clipping after allreduce allows computation to overlap with communication since the clipping is applied, on each GPU, after the final gradients are obtained via communication. However, in terms of sample efficiency (i.e., the number of training samples to reach the same level of training quality), as reported in MLPerf v0.7, gradient clipping before allreduce tends to outperform gradient clipping after allreduce. It is mainly because gradient clipping before allreduce can prevent some problematic mini-batch from having too large impact on the updated parameters. Unfortunately, gradient clipping before allreduce does not allow the overlap of communication and computation. The benefit of better sample efficiency can be offset by the lack of communication/computation overlap. Thus, gradient clipping before allreduce is rarely adopted in large-scale distributed training. In our work, we propose applying both gradient clipping before allreduce and the overlap of computation and communication by performing gradient clipping at the granularity of bucket.

## 4 Proposed Method

### 4.1 Local Presorting with Dataset Stratification

Stratification is a well-known variance reduction technique which assigns samples to groups called strata (groups formed in terms of sequence length in our case) and selects samples in proportion to the probabilities of strata. Figure 3 exemplifies our proposed stratification applied to Wikipedia dataset. We assume batch size of 16 and maximum sequence length of 512. First, we use four strata in terms of sequence length, i.e., stratum 1 contains samples of length from 1 to 128, stratum 2 from 129 to 256, stratum 3 from 257 to 384 and stratum 4 from 385 to 512. As the figure shows, each stratum has its own probability determined by the number of samples belonging to it. For instance, the larger probabilities of strata 1 and 4 exhibit the bi-modal characteristics, i.e., mostly short or long sequences, of Wikipedia dataset. As the figure shows, in our example of local batch size of 16, we can select 5, 2, 3 and 6 samples on strata 1, 2, 3, and 4, respectively. Note that, given the local batch size, the number of selected samples per stratum is determined by the probability of the stratum. As the example shows, the sampling with stratified dataset can ease the load imbalance problem.

We propose applying stratification in a GPU node basis. In the existing method of global presorting [15], presorting across all GPU nodes incurs high communication overhead since it gathers all samples from all the GPU nodes via slow inter-node communication. Our proposed per-GPU node stratification enables us to presort samples only inside of GPU node, which we call *local presorting*, thereby avoiding expensive inter-node communication.

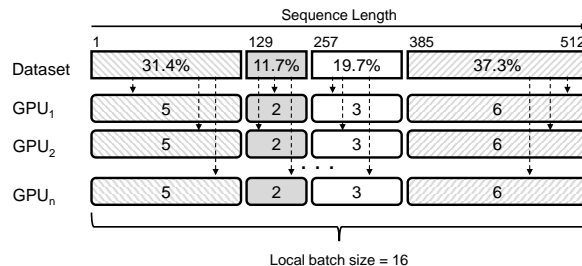


**Figure 3. Example of stratification when dataset is stratified into four strata and batch size is 16.**

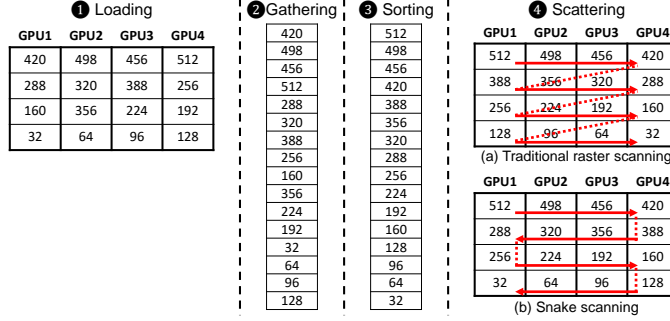


Figure 4. The example of local presorting with two different retrieving patterns: (a) raster and (b) snake scanning.

Figure 4 exemplifies how our local presorting works. We assume a GPU node consists of 4 GPUs and each GPU is initially assigned four samples (four values correspond to their lengths). In the steps of gathering and sorting, we all-gather all the samples inside of a GPU node and sort them. When scattering the presorted samples, we also propose applying a snake pattern scanning as shown in the figure. Compared with the conventional raster scanning, our experiments show the snake pattern proves more effective in mitigating load imbalance.

## 4.2 Bucket-wise Gradient Clipping before AllReduce

Figure 5 (a) and (b) compare how gradient clipping can be applied (a) after and (b) before allreduce under bucket-based synchronization. Gradient clipping after allreduce still enables the overlap of computation and communication. However, gradient clipping before allreduce does not benefit from the overlap. Figure 5 (c) shows how our proposed bucket-wise gradient clipping before allreduce enables the overlap of communication and computation. As shown in the figure, gradients in each bucket are clipped as soon as they are ready and then immediately synchronized with allreduce. Since the clipping is independently applied to each bucket on each GPU, we can transfer buckets of clipped gradients during back-propagation. The pseudocode is provided in the Appendix.

## 5 Experiments

**Experimental environment** We train the BERT model on a large-scale GPU training system consisting of 1,024 NVIDIA A100 GPUs with 100 GB/s network bandwidth. More precisely, the system is a cluster of 128 nodes each of which consists of two AMD EPYC 7543 CPUs and eight NVIDIA 80GB A100 GPUs connected by NVLink and NVSwitch. The servers in the cluster are connected by four HDR 25GB/s Infinibands. We use NVIDIA PyTorch container image, release 21.06 (21.09) for MLPerf v1.1 and (v2.0).

We use automatic hyperparameter optimization tool, Neural Network Intelligence [10], to compare optimizers and gradient clipping methods in a fair way. We use SMAC [3] and reduce the search space by selecting important parameters and exploiting locality in search space as explained in Appendix.

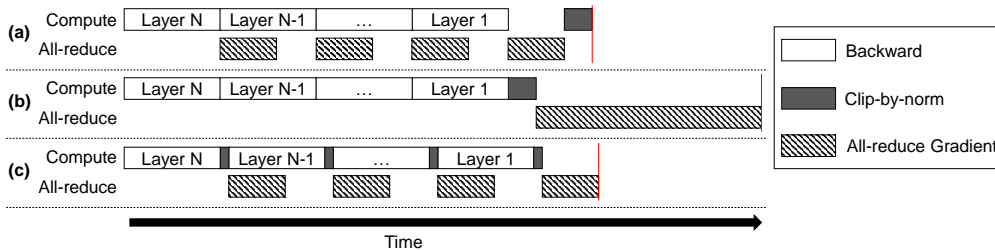


Figure 5. Timeline of gradient clipping methods: (a) gradient clipping after allreduce, (b) gradient clipping before allreduce, and (c) bucket-wise gradient clipping.

**Table 1. Published results from MLPerf Training v1.0 [9], v1.1 [12] and v2.0 [13]**

Version	Vendor	Accelerator	#	Batch size	Results (seconds)	# of samples
v1.0	NVIDIA	NVIDIA A100 GPU	1024	3072	43.5	2.6M~3.0M
	NVIDIA	NVIDIA A100 GPU	4096	12288	19.0	4.7M~5.0M
	Google	TPU-v4	2048	6144	19.1	3.2M~3.4M
	Google	TPU-v4	3456	6912	16.5	3.4M~3.6M
v1.1	NVIDIA	NVIDIA A100 GPU	1024	3072	33.5	2.6M~3.0M
	NVIDIA	NVIDIA A100 GPU	4320	12960	13.6	4.4M~5.0M
	Microsoft	NVIDIA A100 GPU	1024	3072	39.4	2.6M~2.8M
	Microsoft	NVIDIA A100 GPU	2048	6144	25.3	3.2M~3.4M
	<b>Ours</b>	<b>NVIDIA A100 GPU</b>	<b>1024</b>	<b>16384</b>	<b>25.1</b>	<b>2.9M~3.3M</b>
v2.0	NVIDIA	NVIDIA A100 GPU	1024	4096	25.3	2.6M~3.0M
	NVIDIA	NVIDIA A100 GPU	4096	16384	12.4	5.2M~5.9M
	Google	TPU-v4	3456	6912	13.7	4.8M~4.9M
	Google	TPU-v4	4096	14336	11.0	6.5M~6.6M
	<b>Ours</b>	<b>NVIDIA A100 GPU</b>	<b>1024</b>	<b>16384</b>	<b>22.3</b>	<b>2.9M~3.0M</b>

**Table 2. Summary of performance optimization history on 1024 NVIDIA A100 GPUs for MLPerf v1.1**

Optimization Item	Time (sec)	Batch size	# of samples
NVIDIA v1.0 reported	43.5	3K	2.6~3.0M
NVIDIA v1.0 reproduced	59.5	3K	2.6~3.0M
+ PyTorch DDP + ADAM	34.5	16K	3.9~4.3M
+ Bucket-wise gradient clipping	28.9	16K	2.9~3.3M
+ Local Presorting + Stratification	25.1	16K	2.9~3.3M

## 5.1 MLPerf BERT Benchmark Results

Table 1 shows the large-scale training performance of BERT reported in MLPerf Benchmark. Ours ranks the first in the configuration of 1,024 accelerators both in v1.1 and v2.0.

NVIDIA continuously improves the unpadding Fused Multi HEAD Attention (FMHA) kernel [14] and uses different optimization strategy in each benchmark. For load balancing, NVIDIA uses unpadding FMHA kernel and global presorting for small-scale systems ( $\leq 64$  GPUs). They use pad FMHA for large-scale system ( $\geq 1,024$  GPUs) until v1.1 and change to unpad FMHA and packing in v2.0. The gradient clipping method is changed from before allreduce to after allreduce from v1.1.

Our internal optimization history is summarized in Table 2. When we reproduced NVIDIA v1.0 in our system, there was significant performance gap, 43.5 vs 59.5 seconds. The network bandwidth difference (200 vs 100 GB/s) and lack of SHARP (scalable hierarchical aggregation and reduction protocol) affected the performance because the batch size per GPU was very small at 3 and communication and computation was not overlapped due to gradient clipping before allreduce. To overcome this network bandwidth limitation, we first changed the gradient clipping method from before allreduce to after allreduce and tried to increase batch size as much as possible for high GPU utilization. After extensive hyperparameter optimization, we found that conventional ADAM works better than LAMB for large batch training. Then we applied proposed load balancing and gradient clipping method. We used the same method for v2.0 except for updating SW stack such as CUDA, NCCL, and APEX.

## 5.2 Irregular Sequence Length Handling

In this subsection, we evaluate methods for handling irregular sequence lengths. Note that global presorting, packing, and our proposed method are based on unpadding.

**Load balancing effect simulation** First, the effectiveness of load balancing is evaluated by simulation. We basically assume that effective batch size per GPU (local batch size) is 16. We also assume packing ratio 2 for packing, and 8 GPUs per node for our proposed method. In packing/our/other methods, we randomly retrieves 8/16/16 sequences for each GPU from pre-packed/stratified/original dataset, respectively. After retrieving data, we balance them following each

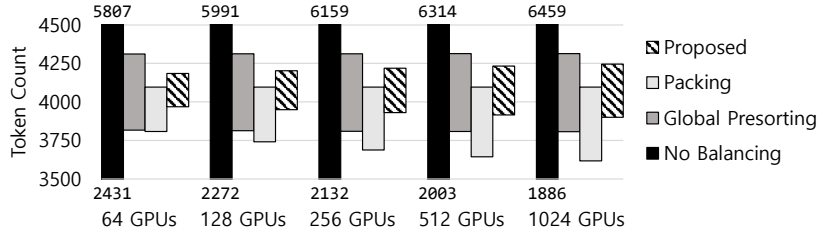


**Figure 6. Average range of token count per GPU for each load balancing method when effective local batch size is 16. The bottom (top) of bar represents the average minimum (average maximum) token count when using the associated load balancing method. The maximum token count of a sequence is 512.**

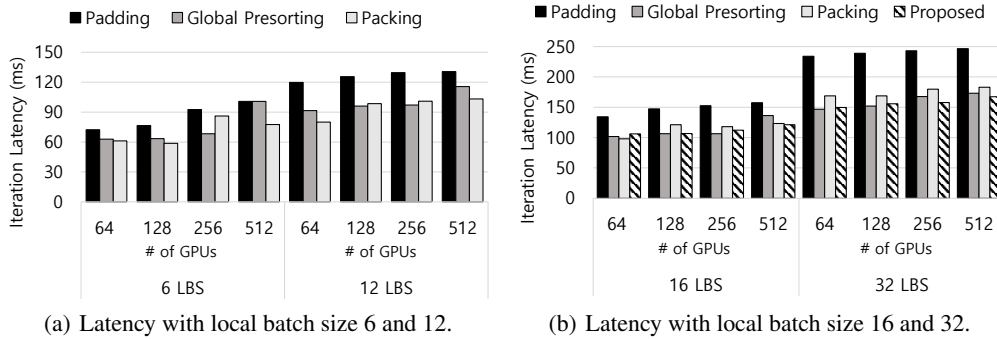


**Figure 7. Latency of each load balancing method with small and large local batch size.**

load balancing method and find maximum and minimum token count processed on a GPU. We repeat the above simulation 100,000 times and calculate average maximum and minimum token count.

Figure 6 depicts the average token count range of each load balancing method, where the shorter bar implies the better balancing. The method of no balancing shows a critical imbalance problem even in 64 GPUs, and the packing method can also suffer from the imbalance problem as the system size grows. In addition, the packing method can also suffer from low utilization due to limited maximum token count. Please refer Appendix for load balancing improvement according to stratification/local presorting/snake scanning step by step.

**End-to-end latency comparison** With padding as the baseline, global presorting, packing and our method are compared in terms of end-to-end latency. Figure 7(a) shows the latency of each method according to the effective local batch size and the number of GPUs. Packing shows good performance when effective local batch size is small (6 and 12) with the help of CUDA graph. The use of CUDA graph by packing is enabled because packing always launches the same FMHA kernel, which is determined by maximum sequence length in the local mini batch. On the other hand, global presorting cannot use CUDA graph acceleration because it needs to launch various FMHA kernels according to the length of sequences to leverage the advantage of the unpadding. Note that we do not evaluate the proposed method with small local batch size because stratification cannot reflect the ratio of strata for small local batch size.

Figure 7(b) shows the training latency of load balancing methods with large batches. When local batch size gets larger than 12, packing could not use CUDA graph like other method because of out-of-memory. Therefore, packing loses advantage over global presorting and global presorting runs faster than packing for most cases. The proposed method gives the lowest latency when the number of GPUs gets larger, because it eliminates communication over all GPUs for load balancing. This result implies that our proposed method is suitable for large batch and large-scale GPU environments.

We also profile the latency for load balancing and calculate its proportion in the total training latency. In case of 1,024 GPUs, the global presorting takes 18.2% of the total training time, while our method takes only 1.9%. Refer to Appendix for detailed analysis of this experiment.

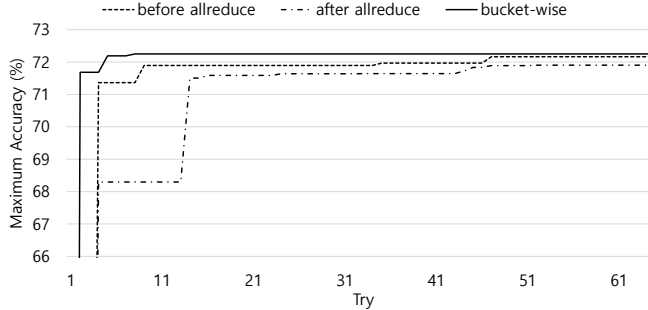


Figure 8. Comparison of hyperparameter optimization cost of gradient clipping methods.

Table 3. MLM accuracy when using each gradient clipping method. Global batch size = 16384, Local batch size = 16, The number of samples = 2.9M

Gradient Clipping Method	Accuracy (%)
Gradient Clipping After Allreduce	72.05
Gradient Clipping Before Allreduce	72.26
Bucket-wise Gradient Clipping	72.25

### 5.3 Gradient Clipping

**Sample efficiency** In this subsection, we compare three gradient clippings: gradient-clipping-after-allreduce, gradient-clipping-before-allreduce, and bucket-wise gradient clipping. First, we compare the sample efficiency by measuring the accuracy for each gradient clipping method after training 2.9 million samples. Because the optimal hyperparameters could be different between gradient clipping methods, the hyperparameters for each method are searched through automated hyperparameter optimization for a fair comparison. Refer to Appendix for the automated hyperparameter optimization methodology for this experiment.

In Table 3, the higher accuracy implies the better sample efficiency. As we discussed in Section 3.2, gradient-clipping-after-allreduce shows lower sample efficiency due to the negative effects of problematic mini-batch having large gradients. On the other hand, bucket-wise gradient clipping method shows high sample efficiency as much as gradient-clipping-before-allreduce, because it reduces the impact of problematic mini-batch effectively as well as gradient-clipping-before-allreduce.

**Hyperparameter optimization cost** In order to compare the cost of finding the optimal hyperparameter for each gradient clipping method, we measure the maximum accuracy according to the number of hyperparameter optimization attempts. For fair comparison, we used Microsoft Neural Network Intelligence (NNI) and SMAC for automatic hyperparameter optimization. In the Figure 8, y-axis means the maximum accuracy achieved over each given number of tries. The figure depicts that bucket-wise gradient clipping requires far fewer attempts to obtain hyperparameters for reasonable accuracy. To achieve the accuracy in Table 3, we have run 9, 66, and 130 tries for bucket-wise gradient-clipping, gradient-clipping-before-allreduce, and gradient-clipping-after-allreduce, respectively.

**Overhead** We also compare the throughput degradation due to gradient clipping methods. We measure the latency of single training iteration under gradient clipping. In Figure 9, we can observe that bucket-wise gradient clipping and gradient-clipping-after-allreduce shows similar latency since both methods well hide the overhead of gradient allreduce. On the other hand, gradient-clipping-before-allreduce shows higher latency because it cannot hide gradient allreduce overhead.

## 6 Discussion and Limitations

**Other parallelisms across transformer based models** The proposed data-parallel training method can be applied together with other parallelisms. For instance, in case of DeepSpeed where model, pipeline and (ZeRO) data parallelisms are utilized, our gradient clipping method can be applied to improve the sample efficiency of data parallelism thereby contributing to fast training.

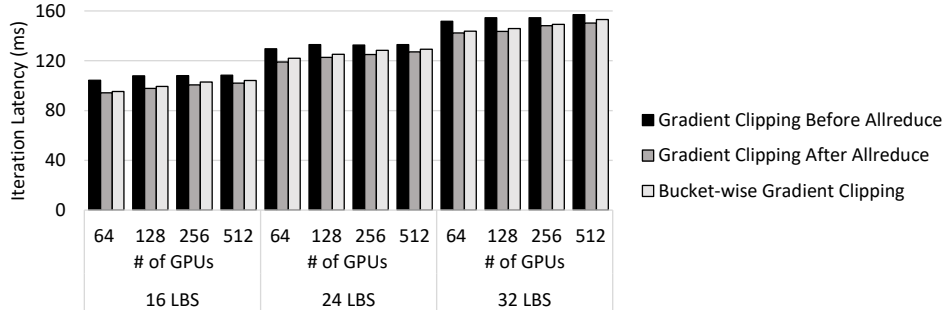


Figure 9. Latency comparison between gradient clipping methods.

**Comparison with previous distributed gradient clipping techniques** M. Liu *et al.* [8] consider a local SGD-type method; since it allows multiple steps of each worker to run before communicating with the others, the local gradient clipping is a natural choice when adopting gradient clipping. If the method aggregates model parameters on all machines after every single step of local updates, this is identical to the gradient-clipping-before-allreduce, which is compared with the proposed bucket-wise gradient-clipping in our paper. In addition, W. Wen *et al.* [22] and Y. Lin *et al.* [7] proposed other gradient-clipping approaches, which can also be categorized in the gradient-clipping-before-allreduce type ones; on the other hand, to the best of our knowledge, our bucket-wise gradient-clipping is the first to combine the advantages of the gradient-clipping-after-allreduce and the gradient-clipping-before-allreduce and take the advantages of both. By doing this, the bucket-wise gradient-clipping allows to overlap communication and computation while achieving an algorithmic efficiency of the gradient-clipping-before-allreduce level.

**Small batch size** Our load balancing method may have a limited utility in case of very small batches (e.g., local batch size of 4) since stratification is based on the probabilities of bins (i.e., strata) and, in case of a very small (e.g., a single) number of samples per bin. In such a case, there is a risk that sampling cannot always reflect the bin statistics. We found that our load balancing becomes effective when the local batch size is 16 where the numbers of per-stratum samples are 5:2:3:6 on four strata, which proves to faithfully reflect the statistics of our training data. On the other hand, bucket-wise gradient clipping is applicable to small batch training since its working unit is a bucket and the number of buckets depends on the model size, not the batch size. We conducted a similar experiment as Table 3 but with a small batch size (256) and hyperparameter from the BERT paper. The proposed method shows higher accuracy (71.76%) than gradient clipping after allreduce (71.56%) after training with the same number of samples.

## 7 Conclusion

We addressed two key issues in large-scale distributed training of BERT models, load balancing and computation/communication overlap. In order to account for the diverse lengths of sentences in the training dataset and to reduce pre-sorting cost, we proposed local presorting based on dataset stratification. We also proposed bucket-wise gradient clipping before allreduce, which enables us to benefit from both gradient clipping before allreduce and the overlap of gradient computation and synchronization. In our cluster of 1,024 NVIDIA A100 GPUs, we report the state-of-the-art training time of 25.1 (22.3) seconds to finish MLPerf BERT training, which is  $1.33\times$  ( $1.13\times$ ) and  $1.57\times$  faster than the other top two (one) submissions to MLPerf v1.1 (v2.0).

## References

- [1] Saurabh Agarwal, Hongyi Wang, Shivaram Venkataraman, and Dimitris Papailiopoulos. On the utility of gradient compression in distributed training systems. *Proceedings of Machine Learning and Systems*, 4:652–672, 2022.
- [2] Mike Barnett, Lance Shuler, Robert van De Geijn, Satya Gupta, David G Payne, and Jerrell Watts. Interprocessor collective communication library (intercom). In *Proceedings of IEEE Scalable High Performance Computing Conference*, pages 357–364. IEEE, 1994.

- [3] Frank Hutter, Holger H Hoos, and Kevin Leyton-Brown. Sequential model-based optimization for general algorithm configuration. In *International Conference on Learning and Intelligent optimization*, 2011.
- [4] Mario Michael Krell, Matej Kosec, Sergio P. Perez, and Andrew Fitzgibbon. Efficient sequence packing without cross-contamination: Accelerating large language models without impacting performance, 2022.
- [5] Alex Krizhevsky. One weird trick for parallelizing convolutional neural networks, 2014.
- [6] Shen Li, Yanli Zhao, Rohan Varma, Omkar Salpekar, Pieter Noordhuis, Teng Li, Adam Paszke, Jeff Smith, Brian Vaughan, Pritam Damania, et al. Pytorch distributed: Experiences on accelerating data parallel training. *VLDB Endowment*, 13(12):3005–3018, 2020.
- [7] Yujun Lin, Song Han, Huizi Mao, Yu Wang, and William J Dally. Deep gradient compression: Reducing the communication bandwidth for distributed training. *arXiv preprint arXiv:1712.01887*, 2017.
- [8] Mingrui Liu, Zhenxun Zhuang, Yunwen Lei, and Chunyang Liao. A communication-efficient distributed gradient clipping algorithm for training deep neural networks. *Advances in Neural Information Processing Systems*, 35:26204–26217, 2022.
- [9] Peter Mattson, Christine Cheng, Gregory Diamos, Cody Coleman, Paulius Micikevicius, David Patterson, Hanlin Tang, Gu-Yeon Wei, Peter Bailis, Victor Bittorf, et al. Mlperf training benchmark. *Proceedings of Machine Learning and Systems*, 2:336–349, 2020.
- [10] Microsoft. Microsoft Neural Network Intelligence. <https://www.microsoft.com/en-us/research/project/neural-network-intelligence>, 2017.
- [11] Microsoft. Deepspeed: Extreme-scale model training for everyone. <https://www.microsoft.com/en-us/research/blog/deepspeed-extreme-scale-model-training-for-everyone>, 2020.
- [12] MLCommons. v1.1 results. <https://mlcommons.org/en/training-normal-11/>, 2021.
- [13] MLCommons. v2.0 results. <https://mlcommons.org/en/training-normal-20/>, 2022.
- [14] NVIDIA. Nvidia apex library. <https://github.com/NVIDIA/apex>.
- [15] NVIDIA. Boosting NVIDIA MLPerf Training v1.1 Performance with Full Stack Optimization. <https://developer.nvidia.com/blog/boosting-mlperf-training-v1-1-performance-with-full-stack-optimization/>, 2021.
- [16] Pranav Rajpurkar, Jian Zhang, Konstantin Lopyrev, and Percy Liang. Squad: 100,000+ questions for machine comprehension of text, 2016.
- [17] Peter Sanders, Jochen Speck, and Jesper Larsson Träff. Two-tree algorithms for full bandwidth broadcast, reduction and scan. *Parallel Computing*, 35(12):581–594, 2009.
- [18] Alexander Sergeev and Mike Del Balso. Horovod: fast and easy distributed deep learning in tensorflow. *arXiv preprint arXiv:1802.05799*, 2018.
- [19] Zhenheng Tang, Shaohuai Shi, Xiaowen Chu, Wei Wang, and Bo Li. Communication-efficient distributed deep learning: A comprehensive survey, 2020.
- [20] Yuichiro Ueno and Rio Yokota. Exhaustive study of hierarchical allreduce patterns for large messages between gpus. In *2019 19th IEEE/ACM International Symposium on Cluster, Cloud and Grid Computing (CCGRID)*, pages 430–439. IEEE, 2019.
- [21] Alex Wang, Amanpreet Singh, Julian Michael, Felix Hill, Omer Levy, and Samuel Bowman. GLUE: A multi-task benchmark and analysis platform for natural language understanding. In *the 2018 EMNLP Workshop BlackboxNLP: Analyzing and Interpreting Neural Networks for NLP*, 2018.
- [22] Wei Wen, Cong Xu, Feng Yan, Chunpeng Wu, Yandan Wang, Yiran Chen, and Hai Li. Terngrad: Ternary gradients to reduce communication in distributed deep learning. *Advances in neural information processing systems*, 30, 2017.
- [23] Wikimedia. Wikimedia downloads. <https://dumps.wikimedia.org>, 2020.

- [24] Yang You, Igor Gitman, and Boris Ginsburg. Large batch training of convolutional networks, 2017.
- [25] Yang You, Jing Li, Sashank Reddi, Jonathan Hseu, Sanjiv Kumar, Srinadh Bhojanapalli, Xiaodan Song, James Demmel, Kurt Keutzer, and Cho-Jui Hsieh. Large batch optimization for deep learning: Training BERT in 76 minutes. In *International Conference on Learning Representations*, 2020.
- [26] Yujia Zhai, Chengquan Jiang, Leyuan Wang, Xiaoying Jia, Shang Zhang, Zizhong Chen, Xin Liu, and Yibo Zhu. Bytetransformer: A high-performance transformer boosted for variable-length inputs. *arXiv preprint arXiv:2210.03052*, 2022.

## A Automatic Hyperparameter Optimization

[3] and [10] explained challenges in fairly comparing optimizers and revealed that hyperparameter tuning protocol is a key determinant of optimizer rankings. Currently, various hyperparameter optimization algorithms such as SMAC [7], TPE [2], BOHB [4], and GP Tuner [11] are available in tools such as Hyperopt [2], Spearmint [11], Autotune [8], Optuna [1], Vizier [5], and Microsoft Neural Network Intelligence (NNI) [9].

However, there is no agreement on how to conduct an experiment that fairly compares learning algorithms. Although it may not be perfect, we perform hyperparameter optimization with the same computation budget when comparing optimizers (ADAM vs LAMB) and gradient clipping methods mentioned in Section 5.3. Among various tools and hyperparameter optimization algorithms, we simply select Microsoft NNI and SMAC because of its popularity, and then try to use computation budget for hyperparameter optimization efficiently by following two approaches:

**Importance-aware search target selection** We measure the importance of hyperparameters by fANOVA [6] values and observe that some hyperparameters such as the ratio between peak and end learning rate (LR),  $\epsilon$ , and LR init<sup>1</sup> have little impact on the training performance. Hence, it is more beneficial to exclude those less-important hyperparameters in the search procedure because of limited time budgets and computation costs. The exclusion of less-important hyperparameters helps us to decrease the dimension of the search space. Table 4 exemplifies the result of hyperparameter optimization.

**Search range reduction of the selected targets** In addition to the selection of search targets, it is also important to properly choose the search ranges of the selected hyperparameters. If the search ranges are too wide, it takes too much time to search optimal hyperparameters. On the other hand, if the search ranges are too narrow, the HPO tools may find suboptimal hyperparameters. In Figure 10, each line stands for combinations of the hyperparameters evaluated by the NNI. The green lines indicate the combinations that show low task performance, whereas the red bold lines indicate the good candidates for the task. As observed in the figure, there exists a cluster that shows high task performance and such a locality allows us to narrow down the search space without the risk of losing optimal points.

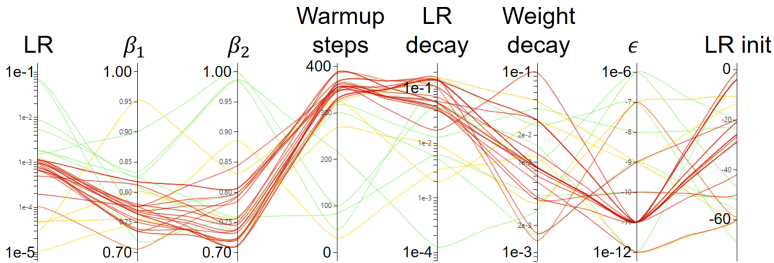


Figure 10. Illustration of hyperparameter searching results.

Table 4. Example of hyperparameter search space reduction. We set hyperparameter optimization budget as 150 and 50 trials for coarse and fine stages, respectively

Hyperparameter	fANOVA	Coarse	Fine
LR	0.50	[1e-5, 1e-1]	[1e-3, 1e-3]
$\beta_1$	0.25	[0.7, 0.999]	[0.7, 0.80]
Weightdecay	0.17	[1e-3, 1e-1]	[1e-2, 1e-1]
$\beta_2$	0.03	[0.7, 0.999]	[0.85, 0.999]
Warmup steps	0.03	[0, 400]	[0, 300]
End LR ratio	0.01	[1e-4, 0.2]	5e-4
$\epsilon$	0.01	[1e-12, 1e-5]	1e-11
LR init	0.00	[-73, 0]	-47

<sup>1</sup>LR init is a coefficient that determines the initial learning rate.

## B Bucket-wise Gradient Clipping Algorithm

Algorithm 1 shows the bucket-wise gradient clipping in detail. Note that the threshold  $c$  is divided by  $B$  to ensure that bucket-wise clipping behaves similarly to whole gradient clipping. We observe training becomes unstable without this.

---

### Algorithm 1 Bucket-wise Gradient Clipping

---

- 1: **Input:** model parameter  $\theta$ , training data  $D$ , minibatch sample  $X$ , number of iteration  $T$ , gradient  $G$ , bucket of gradients  $G_b$ , number of buckets  $B$ , threshold for clip  $c$ , learning rate  $\eta$
- 2:  $\theta \leftarrow$  random initialization
- 3: **for**  $t = 1, \dots, T$  **do**
- 4:   Sample minibatch  $X \subset D$
- 5:   **for**  $b = B, B - 1, \dots, 1$  **do**
- 6:     Compute  $G_b$
- 7:     **if**  $\|G_b\| \geq c/\sqrt{B}$  **then**
- 8:        $G_b \leftarrow c \frac{G_b}{\sqrt{B}\|G_b\|}$
- 9:     **end if**
- 10:     $G_b \leftarrow$  All-Reduce( $G_b$ )
- 11:   **end for**
- 12:    $G \leftarrow [G_1, \dots, G_B]$
- 13:    $\theta \leftarrow ADAM(\theta, \eta, G)$
- 14: **end for**

} Do in parallel

## C Extensive Experiments for Load Balancing

### C.1 Latency

We profile the latency for load balancing and calculate its proportion in the total training latency. We conduct this experiment only for global presorting and the proposed method, because only these two methods have a stage for load balancing. On the other hand, packing uses packed dataset which is prepared before starting training. Figure 11 shows that the load balancing overhead of global presorting becomes larger when more GPUs are used since it requires all GPUs participate in all-gather and sort the gathered samples. The load balancing latency takes 18.2 % of the total training time in case of 1,024 GPUs. On the other hand, in our method, the overhead of load balancing remains constant across different numbers of GPUs since GPUs do not communicate with each other during load balancing time.

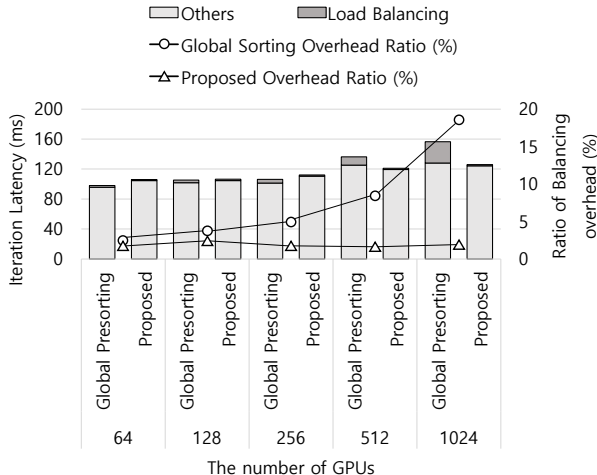


Figure 11. Latency breakdown of global presorting and proposed method. The latency of load balancing is profiled using torch.profiler

## C.2 Balance

Table 5 compares global presorting and our proposed methods according to stratification/local presorting/snake scanning step by step. Combining stratification, local presorting, and snake scanning pattern is required to outperform global presorting.

**Table 5. Load balancing improvement according to stratification/local presorting/snake scanning step by step.**

	Minimum	Maximum
No Balancing	1,886	6,459
+ Stratification	3,620	4,482
+ Local Presorting	3,743	4,401
+ Snake Scanning Pattern	3,900	4,246
Global Presorting	3,807	4,313

## References

- [1] Takuya Akiba, Shotaro Sano, Toshihiko Yanase, Takeru Ohta, and Masanori Koyama. Optuna: A next-generation hyperparameter optimization framework. In *ACM SIGKDD International Conference on Knowledge Discovery & Data Mining*, 2019.
- [2] James Bergstra, Brent Komer, Chris Eliasmith, Dan Yamins, and David D Cox. Hyperopt: A python library for model selection and hyperparameter optimization. *Computational Science & Discovery*, 8(1), 2015.
- [3] Dami Choi, Christopher J. Shallue, Zachary Nado, Jaehoon Lee, Chris J. Maddison, and George E. Dahl. On empirical comparisons of optimizers for deep learning, 2020.
- [4] Stefan Falkner, Aaron Klein, and Frank Hutter. Bohb: Robust and efficient hyperparameter optimization at scale. In *International Conference on Machine Learning*, 2018.
- [5] Daniel Golovin, Benjamin Solnik, Subhodeep Moitra, Greg Kochanski, John Karro, and David Sculley. Google vizier: A service for black-box optimization. In *ACM SIGKDD International Conference on Knowledge Discovery and Data Mining*, 2017.
- [6] Frank Hutter, Holger Hoos, and Kevin Leyton-Brown. An efficient approach for assessing hyperparameter importance. In *International Conference on Machine Learning*, 2014.
- [7] Frank Hutter, Holger H Hoos, and Kevin Leyton-Brown. Sequential model-based optimization for general algorithm configuration. In *International Conference on Learning and Intelligent optimization*, 2011.
- [8] Patrick Koch, Oleg Golovidov, Steven Gardner, Brett Wujek, Joshua Griffin, and Yan Xu. Autotune: A derivative-free optimization framework for hyperparameter tuning. In *ACM SIGKDD International Conference on Knowledge Discovery & Data Mining*, 2018.
- [9] Microsoft. Microsoft Neural Network Intelligence. <https://www.microsoft.com/en-us/research/project/neural-network-intelligence>, 2017.
- [10] Robin M Schmidt, Frank Schneider, and Philipp Hennig. Descending through a crowded valley-benchmarking deep learning optimizers. In *International Conference on Machine Learning*, pages 9367–9376. PMLR, 2021.
- [11] Jasper Snoek, Hugo Larochelle, and Ryan P Adams. Practical bayesian optimization of machine learning algorithms. In *Advances in Neural Information Processing Systems*, 2012.